Monatshefte für Chemie 118, 1011—1029 (1987)

Monatshefte für Chemie
Chemical Monthly

Reactivity of Pyrrole Pigments. Part 10 [1] MINDO/3 Calculations on Bile Pigments

Rosa Caballol[a], Josep M. Ribó*[,b], Francesc R. Trull[b], and Asunción Vallès[b]

[a] Departament de Química Física, Facultat de Química de Tarragona, Universitat de Barcelona, E-43005 Tarragona (Catalunya), Spain

[b] Departament de Química Orgànica, Facultat de Química, Universitat de Barcelona, E-08028 Barcelona (Catalunya), Spain

(Received 1 August 1986. Accepted 14 October 1986)

The applicability of the MINDO/3 method is evaluated for tetrapyrrolic bile pigments: geometries from already calculated dipyrrolic partial models have been used to reduce the calculation time. Net atomic charges and reactivity parameters obtained from the frontier orbital model, i.e. HOMO and LUMO distribution on the molecule, are reported for several conformations.

(Keywords: Bilatrienes-abc; Bile pigments; 2,3-Dihydrobilatrienes-abc; Frontier orbital model; MINDO/3)

Reaktivität von Pyrrolpigmenten, 10. Mitt. MINDO/3-Rechnungen von Gallenpigmenten

Es wird der Einsatz von MINDO/3 für tetrapyrrolische Gallenpigmente beschrieben. Um die Rechenzeit herabzusetzen, wurden geometrische Daten verwendet, die vorher für dipyrrolische Partialstrukturen ermittelt worden waren. Für mehrere Konformationen werden Ladungsdichten und Reaktivitätsparameter nach dem Frontier-Orbital-Modell, nämlich HOMO- und LUMO-Verteilung, berichtet.

Introduction

π-Electron methods have been used as a theoretical tool for the study of tetrapyrrolic bile pigments [2]. More elaborate semi-empirical methods have only been used for simpler dicyclic partial models [3]. In the preceding publication [1] we have evaluated the applicability of the MINDO/3 method [4] to the study of dipyrrolic partial models of bile pigments. Based on these calculations, we report now the MINDO/3 results for the basic structures of three tetrapyrrolic systems (**1–3:** see formula scheme:

The bilatriene-*abc* **1** (verdin) and the two tautomeric forms on the central nitrogens of the 2,3-dihydrobilatrienes-*abc*, i.e. **2** and **3**, that represent the basic structures of the chromophore of some phytobiliproteins (e.g. phytochrome).

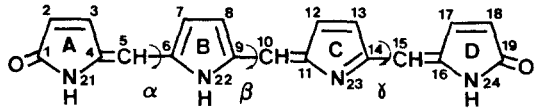

1

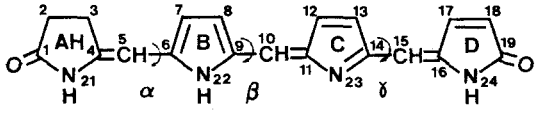

2

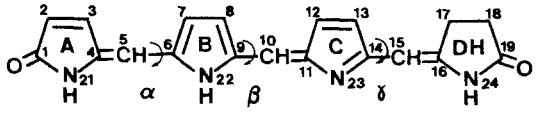

3

For the methodology of the conceptual decomposition of the tetrapyrrolic structure into dipyrrolic partial models—already used by other authors—see the formula scheme and our previous publication [1]. To avoid too long calculation times, the geometrical parameters of the dipyrrolic structures previously calculated [1] were used with the restriction of planarity as before. Optimization was only performed for the C = C exocyclic double bond distances, and their corresponding angles under restriction of planarity. Due to the limitation of the method in the calculation of the total energy for different conformers, as already discussed for dipyrrolic systems [1], these approximations cannot affect the usefulness of the method.

In the calculations of structures with orthogonal rings, fixed geometries were used. Reactivity parameters were calculated from the HOMO and the LUMO atomic orbital coefficients, as we have described before [1]. For more details about the MINDO/3 method see also our preceding paper [1].

Results and Discussion

As in the case of the dipyrrolic partial structures [1], the geometries, the total energies and the difference of energy between conformers calculated by MINDO/3, do not match completely with the experimental data on the geometry and the energy differences between diastereoisomers and between conformational isomers. During the last years many X-ray data about bile pigments have been published [5, 6]. Nowadays, every *a priori* method to be used in bile pigments should be able to explain questions arising from these new experimental data, e.g. in dihydrobilatriene-*abc* systems (**3**) the bond length C 15–C 16 (see formula scheme for numbering) is shorter than in fully unsaturated bilatrienes-*abc* (**1**) [6]. In this sense the MINDO/3 method does not seem to be adequate to reach this goal. The failures observed in the dipyrrolic systems are also observed in the tetrapyrrolic ones.

Calculation of structure **1** (*Z,Z,Z*-isomer) with optimization of the geometrical parameters of the exocyclic double bond system, gives an energy minimum for the helical form, but at diedral angles about 30°–40°, which are higher than the experimental ones [5]. In all the calculated structures the internal angles at the exocyclic carbon atoms are wider (ca. 15°) than the experimental ones. As we have already reported [1], these deviations must be attributed to the enhancement of the non bonded interactions and to the neglect by the MINDO/3 method of the intramolecular hydrogen bonds [7]; the latter point was corroborated through examination of the corresponding bond orders and bicentric energy terms between —N= and H—N.

Nevertheless, the net atomic charge distribution—to our knowledge no published data exist for bile pigments—and the HOMO and LUMO distribution on the molecule (i.e. the reactivity parameters towards electrophiles and nucleophiles; see Ref. [1]), present interesting aspects.

Dipole Moments and Electronic Densities

Table 1 shows, at some selected conformations, the dipole moments calculated by MINDO/3 and also by the vectorial sum of the dipole moments of the one ring partial models (see Ref. [1] for their definition) of the (*Z,Z,Z*)-isomers of **1–3**. The two types of estimated dipole moments are in good agreement, with respect to the scalar values as well as to the vector direction. However, taken into account the above mentioned more open geometry at the exocyclic double bonds in the calculated structures as opposed to the experimental values, these calculated dipole moments could be different from the real ones. In a force field method applied to bile pigments [3 c, 8] the dipole moment was approximated as vectorial

Table 1. *Dipole moments calculated by means of MINDO/3 and calculated by the vectorial sum of the partial dipole moments*[a] *for some conformations of the (Z,Z,Z)-isomers of* **1–3**

Structure (Z,Z,Z)	Conformational angles[b]			MINDO/3 Dipole moment				Dipole moment from vectorial sum			
	α	β	ψ	*D*	Components[c]			*D*	Components[c]		
					x	*y*	*z*		*x*	*y*	*z*
1 (ABCD)	10°	15°	5°	4.63	−4.10	1.87	1.11	4.77	−3.99	2.08	1.59
1 (ABCD)	90°	90°	90°	5.82	0.02	5.37	2.23	6.00	−0.21	5.58	2.19
2 (AHBCD)	10°	15°	5°	3.54	−3.08	1.62	0.67	4.62	−3.77	2.57	0.76
2 (AHBCD)	90°	90°	90°	5.67	−0.72	5.41	1.54	5.87	−0.74	5.57	1.68
3 (ABCDH)	10°	15°	5°	3.85	−3.15	1.89	1.14	4.53	−3.84	2.16	1.06
3 (ABCDH)	90°	0°	90°	2.26	0.92	−0.02	2.06	2.77	0.99	0.12	2.59

[a] See Ref. [1] for the partial dipole moments of the monocyclic models used
[b] See formula scheme for the definition of the angles α, β, and ψ
[c] Coordinate origin at N 24; N 24—C 19 *x* axis; ring D (or DH) on the *xy* plane (see formula scheme)

Table 2. *Correlation analysis corresponding to the regression models (1), (2), and (3) between experimental chemical shifts (^{15}N-, and ^{13}C-NMR) and MINDO/3 net atomic charges*[a] *(see text)*

NMR[b]	Regression model	Regression parameters						
		n	*a*	*b*	*c*	*r*	*s*	*t* or *F*
^{15}N	(1)	4	−228 (± 53)	−141 (± 276)		0.3400	62	0.51
	(2)		−129 (± 23)	−424 (± 129)	−168 (± 46)	0.9688	23	7.6
	(3)		−165 (± 55)	−77 (± 89)		0.5199	56	0.86
^{13}C	(1)	11	122 (± 6)	101 (± 19)		0.8660	15	5.2
	(2)		123 (± 2)	−93 (± 32)	−131 (± 21)	0.9789	6.7	92
	(3)		121 (± 3)	73 (± 7)		0.9560	9.0	9.8

[a] *n* Number of points (chemical shifts or atoms); *r* correlation coefficient; *s* standard deviation of the estimate; *F* value for the significance of the multilinear regression [(2)]; *t Student's t* value for the significance of the linear regression [(1) and (3)]

[b] δ_A^{exp} ^{15}N from Ref. [12]. δ_A^{exp} ^{13}C from Ref. [13]

sum of partial dipole moments of the monocyclic partial models. The results reported here are in agreement with this approximation.

The net atomic charge is an interesting parameter, which could be used in force field methods for the calculation of conformational energies, or in models to calculate the interaction of the bile pigment molecule with a dipole-charge or with a point charge. It is possible to obtain an estimation of the accuracy of the electronic charge distribution predicted in our calculations by correlating the net atomic charges with their experimental NMR chemical shifts. Table 2 shows the regression analysis between the NMR chemical shifts (^{15}N and the ^{13}C) of the structure of 2,3-dihydrobilatriene-*abc* **3** (ABCDH; see formula scheme), and the MINDO/3 net atomic charges: only the quaternary carbon atoms and the exocyclic methine carbon atoms have been considered, because the experimental data available correspond to substituted tetrapyrroles, which have a different electronic charge on the rest of the atoms. The regression models [9, 10] indicated below have been used for such correlations. Table 2 shows the regression analysis for Eqs. (1) and (2) taken from Ref. [10], and Eq. (3) which is not described in the literature. Other equations reported in the literature [10] do not give better correlations than the three shown here.

$$\delta_A = a + b \cdot q_A \tag{1}$$

$$\delta_A = a + b \cdot q_A + c \cdot \sum_B q_B \tag{2}$$

$$\delta_A = a + c \cdot \sum_B q_B \tag{3}$$

δ_A = chemical shift of atom A
q_A = net atomic charge at atom A
q_B = net atomic charge of an atom B directly bonded to atom A
a, b, and c = regression parameters

In the case of the ^{15}N-NMR values [11] good correlation can only be obtained when the charges of the neighbouring atoms are taken into account [i.e. regression model (2)]; see Table 2 and Fig. 1. However, due to the small number of points (4 chemical shift values), these results must be carefully used, as indicated by the low F value.

In the case of the ^{13}C-NMR chemical shifts [12] a good correlation is also obtained through regression model (2). However in this case the use of regression model (3) [$\sum_B q_B$ alone] gives the same significance as regression model (2), which is shown by the good correlation obtained for the Eq. (3), compared to Eq. (2) (see Table 2). These results arise from the good linear correlation existing between q_A and its corresponding $\sum_B q_B$, and from the big charge separation between carbons and heteroatoms linked by a double bond that the MINDO/3 method predicts [13]. The goodness of the MINDO/3 dipole moments must be originated by the $\sum_B q_B$ compensation of the errors on q_A. The linear correlations obtained here corroborate this explanation.

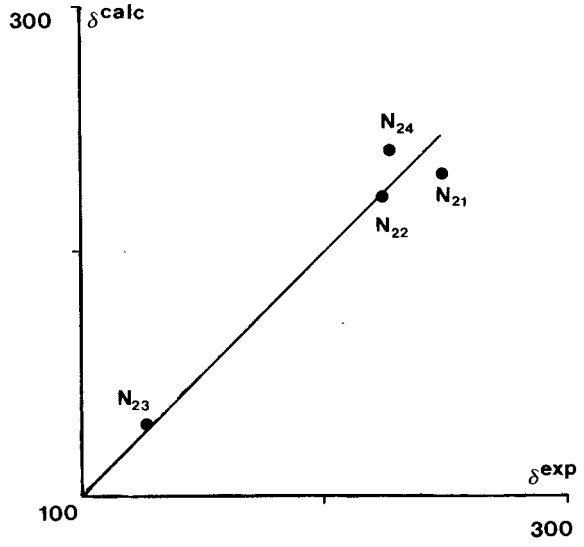

Fig. 1. Plot of δ_A^{exp} vs. δ_A^{calc} for the ^{15}N-NMR signals of **3**; δ_A^{calc} are predicted by the regression model (2) (see text and Table 2)

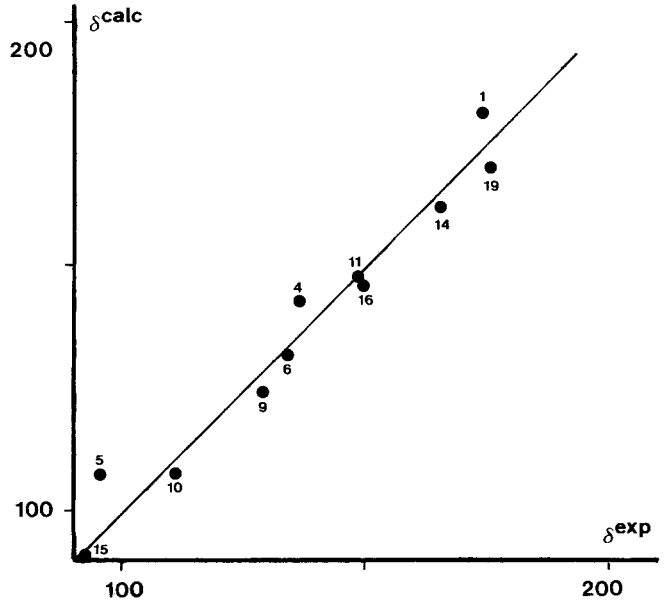

Fig. 2. Plot of δ_A^{exp} vs. δ_A^{calc} for the ^{13}C-NMR signals of sp^2 quaternary carbon atoms of **3**; δ_A^{calc} are predicted by the regression model (2) (see text and Table 2)

Table 3. *Net atomic charges for the structures* **1**, **2**, *and* **3** *(Z,Z,Z-isomer, see text), at the syn,syn,syn conformation* $\alpha = 20°$, $\beta = 10°$, $\psi = 20°$ *(see formula scheme): in parenthesis the limits of variation when changing the conformational angle (from 0° to 180°)*

Atom[a]	Structure		
	1	**2**	**3**
O—C 1	−0.544 (−0.548 − −0.540)	−0.540 (−0.542 − −0.538)	−0.539 (−0.549 − −0.539)
C 1	0.641 (0.641 − 0.638)	0.617 (0.617 − 0.613)	0.639 (0.640 − 0.638)
N 21	−0.212 (−0.216 − −0.210)	−0.197 (−0.200 − −0.196)	−0.212 (−0.215 − 0.210)
H—N 21	0.088 (0.092 − 0.082)	0.086 (0.092 − 0.084)	0.083 (0.092 − 0.082)
C 2	−0.146 (−0.152 − −0.144)	−0.065 (−0.065 − −0.064)	−0.148 (−0.154 − −0.145)
H—C 2	0.048 (0.048 − −0.047)	0.016 (0.019 − 0.016)	0.046 (0.046 − 0.40)
H′—C 2	−	0.022 (0.018−0.011)	−
C 3	0.034 (0.038 − 0.030)	0.063 (0.064 − 0.058)	0.034 (0.038 − 0.030)
H—C 3	0.019 (0.021 − 0.018)	−0.017 (−0.017 − −0.013)	0.018 (0.022 − 0.018)
H′—C 3	−	−0.011 (−0.016 − −0.011)	−
C 4	0.109 (0.126 − 0.095)	0.101 (0.118 − 0.088)	0.107 (0.127 − 0.094)
C 5	−0.057 (−0.059 − −0.044)	−0.089 (−0.092 − −0.076)	−0.055 (−0.059 − −0.041)
H—C 5	−0.003 (−0.016 − 0.003)	0.001 (−0.016 − 0.001)	−0.007 (−0.019 − −0.004)
C 6	0.062 (0.063 − −0.045)	0.074 (0.078 − 0.058)	0.061 (0.064 − 0.043)
C 7	−0.096 (−0.110 − −0.083)	−0.105 (−0.113 − −0.093)	−0.093 (−0.106 − −0.083)
H—C 7	0.024 (0.024 − 0.023)	0.024 (0.024 − 0.022)	0.023 (0.024 − 0.022)
C 8	−0.081 (−0.099 − −0.072)	−0.076 (−0.096 − −0.072)	−0.085 (−0.106 − −0.083)
H—C 8	0.030 (0.035 − 0.030)	0.028 (0.031 − 0.028)	0.031 (0.024 − 0.022)
C 9	0.030 (0.044 − 0.019)	0.023 (0.036 − 0.016)	0.037 (0.047 − 0.023)

N 22	0.038 (0.046 – 0.039)	0.036 (0.043 – 0.035)	0.036 (0.044 – 0.036)
H—N 22	0.049 (0.049 – 0.042)	0.047 (0.048 – 0.039)	0.047 (0.050 – 0.040)
C 10	0.027 (0.046 – 0.019)	0.033 (0.040 – 0.026)	0.016 (0.027 – 0.012)
H—C 10	−0.013 (−0.040 – −0.013)	−0.016 (−0.032 – −0.016)	−0.018 (−0.029 – −0.014)
C 11	0.078 (0.100 – 0.069)	0.073 (0.099 – 0.066)	0.086 (0.107 – 0.072)
C 12	−0.010 (−0.014 – −0.004)	−0.009 (−0.015 – −0.003)	−0.012 (−0.016 – −0.006)
H—C 12	0.011 (0.011 – 0.007)	0.006 (0.011 – 0.006)	0.006 (0.009 – 0.006)
C 13	−0.080 (−0.091 – −0.075)	−0.081 (−0.088 – 0.077)	−0.082 (−0.093 – −0.076)
H—C 13	0.011 (0.013 – 0.008)	0.010 (0.012 – 0.010)	0.010 (0.012 – 0.006)
C 14	0.204 (0.206 – 0.195)	0.200 (0.206 – 0.198)	0.220 (0.220 – 0.212)
N 23	−0.234 (−0.234 – −0.207)	−0.232 (−0.223 – −0.198)	−0.247 (−0.247 – 0.219)
C 15	−0.091 (−0.094 – −0.077)	−0.088 (−0.092 – −0.078)	−0.129 (−0.130 – 0.117)
H—C 15	0.012 (−0.012 – −0.003)	−0.002 (−0.005 – 0.002)	−0.002 (0.009 – −0.002)
C 16	0.148 (0.148 – 0.127)	0.145 (0.151 – 0.126)	0.146 (0.148 – 0.120)
C 17	0.030 (0.037 – 0.029)	0.031 (0.037 – 0.029)	0.050 (0.057 – 0.050)
H—C 17	0.012 (0.012 – 0.010)	0.012 (0.013 – 0.010)	−0.013 (−0.016 – −0.009)
H′—C 17	–	–	−0.011 (−0.015 – −0.009)
C 18	−0.145 (−0.152 – −0.145)	−0.146 (−0.153 – −0.146)	−0.066 (−0.067 – −0.066)
H—C 18	0.056 (0.056 – 0.054)	0.056 (0.056 – 0.055)	0.018 (0.021 – 0.019)
H′—C 18	–	–	0.023 (0.023 – 0.018)
N 24	−0.216 (−0.220 – −0.216)	−0.216 (−0.218 – −0.216)	−0.200 (−0.205 – −0.199)
H—N 24	0.089 (0.093 – 0.088)	0.089 (0.096 – 0.087)	0.095 (0.101 – 0.091)
C 19	0.640 (0.640 – 0.638)	0.641 (0.641 – 0.639)	0.614 (0.614 – 0.615)
O—C 19	−0.541 (−0.541 – −0.535)	−0.540 (−0.541 – −0.536)	−0.524 (−0.538 – −0.532)

[a] See formula scheme

For the models of the terminal rings of bile pigments MNDO gives similar dipole moments than MINDO/3, but different net atomic charges. The more significant difference between both methods is observed at the C=O groups: e.g. for the unsaturated terminal ring 3,4-dimethyl-5-methylene-3-pyrrolin-2-one [3 e, 14], MINDO/3 gives C = + 0.62, and O = —0.55, while MNDO predicts C = + 0.37, and O = —0.32, the two calculated dipole moments being very similar, 3.8 D and 3.5 D respectively. The is not a clear advantage of MNDO over MINDO/3 [3 e, 14], because the first method gives ring geometries for the monocyclic systems (e.g. A) with strong out-of-plane distorsions, not so good charge separations for hydrogen atoms bonded to N, and not so good reactivity parameters (i.e. HOMO and LUMO distributions) [3 e, 14].

Table 3 shows the MINDO/3 net atomic charges on each atom for the (*Z,Z,Z*)-isomer of **1–3** at $\alpha = 20°$, $\beta = 10°$, $\psi = 20°$, and the limit of the variation of these charges with the conformational angle for the three calculated structures: all the combinations of planar and perpendicular structures were calculated for the *Z,Z,Z*-isomers (see below). These atomic charges change only slightly with the conformational angle. In fact they are practically the same for *anti* and *syn* conformations and *E* and *Z* configurations. These results mean that parametrization of the net atomic charge of the atoms of bile pigments could be obtained from MINDO/3, or MNDO. Another indication that can be extracted from Table 3 is about the kinetic behaviour towards electrophiles of the nitrogen atoms in charge-controlled reactions. The calculations give as the more negative nitrogen that of pyrrolenin type (N 23) of structure **3** (ABCDH). The negative charge of this atom decreases when its ring is rotated out of the plane of the rest of the molecule. The difference observed in the charge of this nitrogen between structure **3** (ABCDH), where the azafulvene ring is linked to the saturated terminal ring, and structures **2** (AHBCD) and **1** (ABCD), where the azafulvene ring is linked to an unsaturated terminal ring, could be a significant feature of structure **3**, which represents the fundamental structure of the phytochrome chromophore and of other biliproteins. On the other hand, this basic nitrogen shows reactivity parameters near to zero for orbital-controlled reactions towards electrophiles (see below).

Reactivity Parameters and HOMO and LUMO Distribution on the Molecule

The calculated reactivity parameters for the three structures **1–3**, depend—as in the case of the dipyrrolic models [1]—on the angle between the ring systems but are not significantly different between *syn* and *anti* conformations and are also practically independent of the double bond configuration. We have performed the calculation of some isomers with double bonds in the *E* configuration, and in these cases the net atomic

charges, and the reactivity parameters (i.e. HOMO and LUMO atomic orbital coefficients) were practically the same as in the *Z* isomers for the same conformational angle. Small conformational changes affect only slightly the reactivity parameters i.e. the HOMO and LUMO relative distribution on the atoms. Consequently, the reactivity parameters of the all *Z*, all *syn* forms of **1–3**, at $\alpha = 20°$, $\beta = 10°$, $\psi = 20°$, given here must be considered also as the reactivity parameters of all the planar forms of **1–3**, i.e. at any configuration of the double bonds, and for α, β, and ψ angles of ca. 0° or ca. 180°.

Although according to our calculations the reactivity (regardless of steric effects) of almost planar (α, β, $\psi = \pm 20°$) stretched or helical forms is similar, it must be taken into account, as it has been shown for the partial models, that the (*E*)-isomers occur with higher conformational angles than the (*Z*)-isomers. This tendency of higher conformational angles for the (*E*)-isomer exists also in the systems substituted at the exocyclic double bond (e.g. see Ref. [15]). Furthermore, when relating the reactivity parameters reported here with experimental reactivity data, it must be kept in mind that the experimentally studied compounds are alkyl substituted at the β carbon atoms of the rings.

The experimental results described in the literature for the compounds related to structures **1** and **3** can be considered as corresponding to almost planar structures. No experimental data exist about structures of type **2**, because compounds with the structure of tautomer **2** have probably not been isolated. The most stable tautomer of the 2,3-dihydrobilatrienes-*abc* in the *Z,Z,Z*-helical form is represented by structure **3** [16]. We attribute to tautomer **3** the experimental results on 2,3-dihydrobilatrienes-*abc* described in the literature, although it cannot be excluded that the less stable tautomer **2** can also intervene as a reaction substrate.

The experimental reactivity of verdins [**1**; (ABCD)] towards electrophiles (deuteriation, nitration, bromination), with alkyl substituents on the ring carbon atoms is in agreement with the reactivity parameter at the meso exocyclic carbon atoms [3 j, 17] of the "planar" system (see Scheme 1).

The high electrophilicity calculated for the meso carbon atom C 10 in the "planar" structures of **1–3** is also in agreement with the described high reactivity towards several nucleophiles of this carbon atom in compounds with structure of type **1** and **3** [18, 19]. Another experimental result in accordance with our calculations is the internal nucleophilic attack to the methylene-substituted carbon atom of the saturated lactam ring (C 16), reported for the structure of type **3** [20].

On the other hand, the MINDO/3 reactivity parameters towards electrophiles and nucleophiles reported here are in agreement with the more reactive atoms estimated by π-electron methods [2 e, h]. However, the total LUMO and HOMO distribution shows some differences with the results reported in the literature: it seems that MINDO/3 emphasizes the location on the molecule of these two orbitals. As it is shown in

Scheme 1

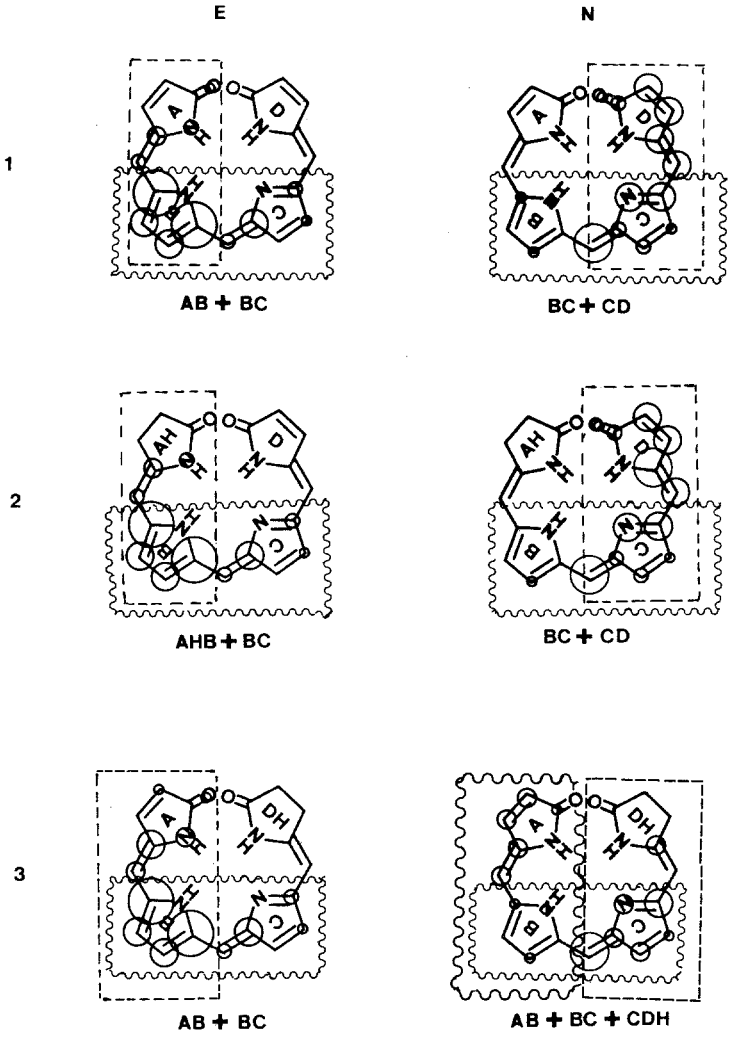

Scheme 1, the reactivity parameters of the planar structure of **1** and **2** are very similar. The electrophilic reactivity estimated for **3** (ABCDH) is also similar to that of **1** and **2**, but the reactivity towards nucleophiles, i.e. the LUMO relative location on the molecule, is very different from the location pattern obtained for **1** (ABCD) and **2** (AHBCD) (see Scheme 1): In spite of this different LUMO location pattern the more reactive position of "planar" **3** towards electrophiles is also carbon atom C 10.

The comparison of these reactivity parameters with those of the implicated dipyrrolic systems shows that for **1–3** the HOMO location—i.e. reactivity towards electrophiles—can be considered as made up of sub-units such as the systems of pyrromethenone (AB or AHB) and pyrromethene (BC). On the other hand, the nucleophilic reactivity—LUMO location—of **1** (ABCD) and **2** (AHBCD) is made up of the LUMO of the two partial models BC and CD, while in the case of **3** (ABCDH) the LUMO can be represented by the addition of the three partial models AB, BC, and CDH (see Scheme 1). Table 4 shows the linear correlations, and their corresponding regression analysis, between the reactivity parameters of the tetrapyrrolic structures and the reactivity parameters of the implicated dipyrrolic partial models (see Ref. [1] for the reactivity parameters of the dipyrrolic systems). The values shown in Table 4 are all statistically very significant in front of any other combination of partial models.

The results of Table 4 were achieved as follows: every linear tetrapyrrolic structure was considered as being made up by a combination of a maximum of three dipyrrolic sub-units (see reference [1] for its definition and reactivity parameters values); only planar or perpendicular structures were taken into account. Analysis was performed according to the following multilinear regression model:

$$y_i^{(\text{tetra})} = a + b\, y_i^{(di.\,1)} + c\, y_i^{(di.\,2)} + d\, y_i^{(di.\,3)} \tag{4}$$

y_i being the reactivity parameter on the atom i; supraindices indicate the corresponding system; a, b, and c are the regression parameters determined by the regression analysis.

In every case a given explanatory variable (i.e. reactivity parameter set) has been included in the correlation, only if the significance level [21] for its introduction turns out to be more than 90%.

In the planar conformers of **1–3** (i.e. for both the helical and the stretched conformations with dihedral angles not far from the plane) it is shown that the HOMO of **1–3** are represented by equal weight of only two (AB and BC) of the three dipyrrolic partial models: the LUMO of **3** is represented by similar weights of the three dipyrrolic systems (AB, BC, and CDH), and the LUMO of **1** and **2** are represented by different weights of two dipyrrolic partial models (BC, and CD or CDH).

The structures with one or several orthogonal rings obviously show strong changes on the HOMO and the LUMO location on the molecule, as it was already observed for the dipyrrolic partial models [1]. Table 4 shows also the reactivity parameters for all the combinations of the structures **1–3** having orthogonal rings. Our preceding publication [1] indicated that in the orthogonal dipyrrolic partial models (here symbolized by e.g. AB 90, CDH 90, . . .) HOMO and LUMO are often almost exclusively located in one of the rings, with the corresponding influence of the other ring which acts as a substituent; e.g. the reactivity towards electrophiles of the 90° conformer of pyrromethenone is practically the

Table 4. *Correlation analysis of the reactivity parameters (*E *towards electrophiles, and* N *towards*

Confor-mational angle α, β, ψ	Structure	React. param.	*a*	Values of the regres *b, c* AB	AHB	BC
20°, 10°, 20°	**1** (ABCD)	E	1.39 (± 0.04)	0.37 (± 0.04)		0.44 (± 0.03)
		N	1.53 (± 0.42)			0.21 (± 0.02)
	2 (AHBCD)	E	1.47 (± 0.44)		0.38 (± 0.04)	0.44 (± 0.03)
		N	0.35 (± 0.29)			0.19 (± 0.02)
	3 (ABCDH)	E	1.63 (± 0.47)	0.39 (± 0.04)		0.40 (± 0.03)
		N	0.81 (± 0.58)	0.30 (± 0.03)		0.29 (± 0.04)
90°, 0°, 0°	**1** (ABCD)	E	0.13 (± 0.29)			0.82 (± 0.02)
		N	0.26 (± 0.30)			0.15 (± 0.02)
	2 (AHBCD)	E	0.25 (± 0.27)			0.81 (± 0.01)
		N	0.21 (± 0.32)			0.14 (± 0.02)
	3 (ABCDH)	E	0.16 (± 0.27)			0.80 (± 0.01)
		N	0.63 (± 0.46)			0.32 (± 0.04)
0°, 90°, 0°	**1** (ABCD)	E	0.15 (± 0.24)	0.90 (± 0.03)		
		N	0.03 (± 0.22)			
	2 (AHBCD)	E	0.19 (± 0.22)		0.89 (± 0.02)	
		N	0.00 (± 0.19)			
	3 (ABCDH)	E	0.17 (± 0.23)	0.89 (± 0.03)		
		N	0.36 (± 0.26)			
0°, 0°, 90°	**1** (ABCD)	E	0.69 (± 0.42)	0.49 (± 0.03)		0.41 (± 0.03)
		N	0.60 (± 0.55)	0.52 (± 0.03)		0.41 (± 0.03)
	2 (AHBCD)	E	0.74 (± 0.48)		0.48 (± 0.04)	0.42 (± 0.03)
		N	0.09 (± 0.41)		0.09 (± 0.02)	0.87 (± 0.02)
	3 (ABCDH)	E	0.68 (± 0.43)	0.49 (± 0.04)		0.41 (± 0.03)
		N	0.50 (± 0.51)	0.59 (± 0.03)		0.35 (± 0.03)
90°, 90°, 0°	**1** (ABCD)	E	0.37 (± 0.28)			
		N	0.16 (± 0.23)			
	2 (AHBCD)	E	0.38 (± 0.28)			
		N	0.07 (± 0.20)			
	3 (ABCDH)	E	0.41 (± 0.28)			
		N	0.64 (± 0.54)			
0°, 90°, 90°	**1** (ABCD)	E	0.19 (± 0.26)	0.89 (± 0.03)		
		N	−0.03 (± 0.11)	0.99 (± 0.12)		
	2 (AHBCD)	E	0.19 (± 0.22)		0.89 (± 0.02)	
		N	0.04 (± 0.06)			
	3 (ABCDH)	E	0.19 (± 0.26)	0.89 (± 0.03)		
		N	−0.06 (± 0.14)	1.01 (± 0.01)		
	1 (ABCD)	E	0.02 (± 0.26)			0.97 (± 0.02)
		N	0.16 (± 0.28)			0.96 (± 0.02)
	2 (AHBCD)	E	0.01 (± 0.29)			0.96 (± 0.02)
		N	0.13 (± 0.26)			0.96 (± 0.02)
	3 (ABCDH)	E	0.02 (± 0.24)			0.96 (± 0.01)
		N	0.09 (± 0.08)			
90°, 90°, 90°	**1** (ABCD)	E	0.34 (± 0.26)			
		N	0.42 (± 0.31)			
	2 (AHBCD)	E	0.36 (± 0.29)			
		N	0.37 (± 0.06)			
	3 (ABCDH)	E	0.37 (± 0.28)			
		N	0.31 (± 0.23)			

[a] For the reactivity parameters of the dipyrrolic structures see Ref. [1]: dipyrrolic models are indicated in the table by the letters of the rings from which they are made up; orthogonality is indicated by the number 90

nucleophiles) between the tetrapyrrolic structures **1–3** *and their dipyrrolic partial models*[a]

sion parameters or d				Regression analysis		
CD	CDH	BC 90	Others	s	r	F or t
				1.84	0.984	338
0.61 (± 0.03)				1.56	0.980	270
				1.85	0.985	365
0.76 (± 0.02)				1.07	0.993	825
				1.93	0.982	291
	0.29 (± 0.05)			1.90	0.966	99
0.14 (± 0.02)				1.05	0.996	1 422
0.82 (± 0.02)				1.10	0.994	854
0.13 (± 0.02)				0.98	0.997	1 612
0.83 (± 0.02)				1.19	0.993	734
	0.16 (± 0.02)			1.02	0.996	1 443
	0.58 (± 0.04)			1.91	0.986	389
		0.06 (± 0.02)		1.01	0.996	1 786
0.88 (± 0.02)		0.11 (± 0.01)		0.82	0.997	1 737
		0.07 (± 0.02)		0.94	0.998	2 277
0.91 (± 0.01)		0.08 (± 0.01)		0.72	0.998	2 344
		0.07 (± 0.02)		0.97	0.997	1 958
	0.78 (± 0.03)	0.17 (± 0.02)		1.11	0.996	1 398
				1.75	0.988	461
				1.86	0.960	179
				2.02	0.985	367
				1.48	0.992	697
				1.79	0.988	434
				1.73	0.978	238
		0.58 (± 0.11)	0.33 (± 0.11) AB 90	1.31	0.997	2 140
0.88 (± 0.22)		0.10 (± 0.01)		0.87	0.996	1 528
		0.47 (± 0.11)	0.44 (± 0.10) AHB 90	1.29	0.998	2 201
0.91 (± 0.01)		0.08 (± 0.01)		0.74	0.998	2 208
		0.59 (± 0.11)	0.31 (± 0.11) AB 90	1.31	0.997	2 144
	0.77 (± 0.03)		0.13 (± 0.03) AB 90	1.89	0.982	292
		0.06 (± 0.02)		1.10	0.996	1 537
				0.50	0.999	132
		0.07 (± 0.02)		0.94	0.998	2 277
			1.00 (± 0.02) CD 90	0.29	0.999	266
		0.0 (± 0.02)		1.09	0.996	1 537
				0.58	0.999	114
				1.13	0.997	60
				1.17	0.996	53
				1.26	0.996	53
				1.12	0.996	56
				1.02	0.997	65
			0.99 (± 0.00) AB 90	0.35	1.000	213
		0.59 (± 0.10)	0.34 (± 0.10) AB 90	1.22	0.998	2 523
		0.53 (± 0.02)	0.41 (± 0.02) AB 90	1.14	0.992	661
		0.49 (± 0.11)	0.43 (± 0.11) AHB 90	1.32	0.997	2 124
			1.00 (± 0.00) CD 90	0.29	1.000	266
		0.58 (± 0.11)	0.33 (± 0.11) AB 90	1.31	0.997	2 140
		0.29 (± 0.01)	0.66 (± 0.01) AB 90	0.84	0.993	1 593

reactivity of a pyrrole ring, but with non symmetrical values because of the effect of the methylenpyrrolinone substituent at the carbon atoms of the pyrole ring. In some of the combinations of Table 4 the relative weights of the implicated partial models are very different. From a simple point of view, some of the combinations of Table 4 can be considered as represented by the HOMO or LUMO of only one partial model, dipyrrolic or even approximately monopyrrolic [e.g. HOMO of **3** (90°, 90°, 0°)]. Only the LUMO of the "planar" **3** must be represented by linear combination of three partial models (see Table 4 and Ref. [1]).

Other interesting general trends can be extracted from Table 4. The HOMO location is always in a partial model that contains the pyrrole ring (B). Violin type conformations (α, β, ψ: 90°, 0°, 0° or 0°, 0°, 90°) have the HOMO and the LUMO on some of the partial models belonging to the three-ring conjugated system. A twist around the central meso bridge-single bond (0°, 90°, 0°) locates the HOMO on the pyrromethenone (AB or AHB) and the LUMO on the other half of the molecule (CD or CDH). In structures with two orthogonals dihedral angles, the remaining dipyrrole planar system prevails, however the HOMO is fundamentally located on the pyrrole ring even if this ring does not belong to the dipyrrole planar system; the LUMO of structure **3** at 90°, 0°, 90° is located on the unsaturated lactam ring A (but on system BC in structures **1** and **2** at the same conformational angles). For structures with four non-conjugated rings (90°, 90°, 90°), the HOMO is always on the pyrrole ring, and the LUMO of **1** and of **3** belong to a π-system located on the non directly bonded rings A and C, however the LUMO of **2** is only on the unsaturated lactam ring (D), which has the azafulvenic ring acting as a substituent (this is also observed for **2** at 0°, 90°, 90°). At this respect DH ring is very different than ring D.

This simple description of the HOMO and LUMO location on the tetrapyrrolic structures of bile pigments is also in agreement with some other experimental results and with the results of π-electron methods on oscillator strengths of the lower energy transition (HOMO—LUMO transition). The variation of the ratio between the intensities of the two main absorption bands is an already established criterion to distinguish between stretched and compact conformations of tetrapyrrolic bile pigments [1 a, 22]: stretched structures are characterized by an increase of the low energy band. This criterion is supported by experimental evidence [23, 24]. Simple calculations from the HOMO and LUMO values reported here give oscillator strengths in agreement with that evidence. The compact helical structure [(*Z*,*Z*,*Z*)-20°, 10°, 20°] of **1** gives, in our case, a calculated oscillator strength value for the HOMO—LUMO transition in a ratio of 1 : 3 with the same transition calculated for the stretched structure [(*Z*,*E*,*Z*)-180°, 180°, 180°]. It is graphically shown in Scheme 2 how dif-

Scheme 2

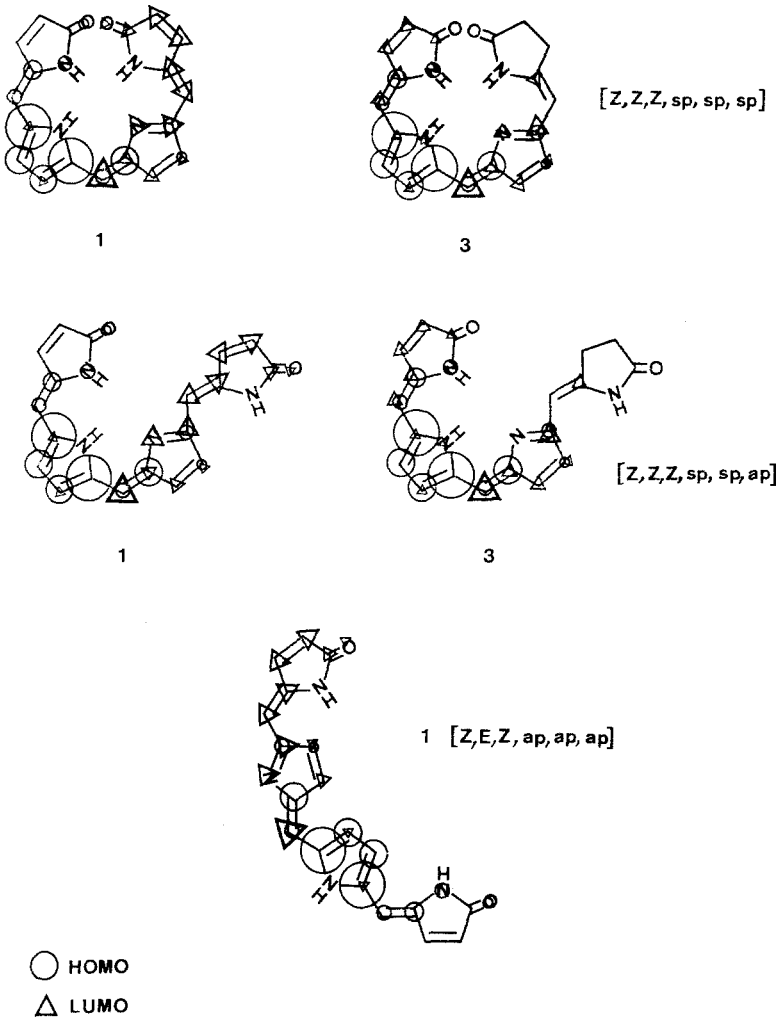

ferently located in space are the HOMO and the LUMO in these two forms: the increase in transition dipole moment when going from the compact to the stretched (the corresponding atomic orbital coefficients being approximately the same for both structures) must be attributed to the HOMO—LUMO relative positions in space.

PPP-Calculations on structures of type **3** show also that practically no effect is produced upon the oscillator strength, when going from the compact to the stretched form, by rotation of the system CDH [2 h]; our

calculations indicate that the ratios between the oscillator strengths of [(*Z,Z,Z*)-20°, 10°, 20°] and [(*Z,Z,Z*)-0°, 0°, 180°] for **1** and **3** are 1.81 and 1.26 respectively; Scheme 2 shows how in structure **3** this change on the relative position of ring CDH practically does not affect the location in the space of HOMO and LUMO, contrarily to what happens in **1** when moving sub-unit CD.

Furthermore this HOMO and LUMO distribution also accounts for the polarization of the low energy band of the electronic spectra of (*Z,Z,Z*; *sp, sp, sp*)-bilatrienes-*abc* of type **1** (see Ref. [25] for an experimental determination).

A self-evident statement arises from the calculations reported here: a verdin system is not a good model for the chromophore group of the phytochrome; the appropriate model must be a 2,3-dihydro system. A second statement refers to how important it is to know the corresponding tautomeric equilibrium involving the nitrogen atoms N 22 and N 23 for any conformation.

We are very grateful to Dr. *P. Segura* for his comments on the correlation analysis.

This work is part of the CAICYT research project 459/84. The calculations were carried out using an IBM-3083/X computer at the "Centre de Càlcul de la Universitat de Barcelona" and a DEC VAX 11-750 computer purchased with funds provided by the CAICYT (grant 657/81).

References

[1] Part 9: *Caballol R, Ribó JM, Trull FR, Vallés A* (1987) Monatsh Chem 118: 993

[2] a) *Burke MJ, Pratt DC, Moscowitz A* (1972) Biochemistry 11: 4025; b) *Chae Q, Song P-S* (1975) J Am Chem Soc 97: 4176; c) *Sugimoto T, Oishi M, Suzuki H* (1977) J Phys Soc Japan 43: 619; d) *Wagniere G, Blauer G* (1976) J Am Chem Soc 98: 7806; e) *Falk H, Höllbacher G* (1978) Monatsh Chem 109: 1429; f) *Scheer H, Formanek H, Schneider S* (1982) Photochem Photobiol 36: 259; g) *Scharnagl C, Köst-Reyes E, Schneider S, Köst HP, Scheer H* (1983) Z Naturforsch 38 c: 951; h) *Falk H, Gsaller H, Hubauer E, Muller N* (1985) Monatsh Chem 116: 939

[3] a) *Falk H, Hofer O* (1974) Monatsh Chem 105: 995; b) *Favini G, Pitea D, Manitto P* (1979) Nouv J Chim 3: 299; c) *Falk H, Höllbacher G, Hofer O, Muller N* (1981) Monatsh Chem 112: 391; d) *Ribó JM, Masip MD, Vallès A* (1981) Monatsh Chem 112: 359; e) *Ribó JM, Vallès A* (1983) J Chem Res (S) 1983: 84 (M) 2501; f) *Cetina R, Rubio M, Salmón M, Bernal J* (1978) Aust J Chem 31: 1911; g) *Salmón M, Rubio M, Cetina R* (1981) J Heterocyc Chem 18: 837; h) *Rubio M, Cetina R, Salmón M* (1982) Rev Roum Chim 27: 285; i) *Rubio M, Cetina R, Fuentes-Martinez GJ* (1984) Afinidad 41: 164; j) *Daroca A, Mercè R, Ribó JM, Trull FR, Vallès A* (1984) Monatsh Chem 115: 357

[4] *Bingham RC, Dewar MJS, Lo DH* (1975) J Am Chem Soc 97: 1285

[5] *Sheldrick WS* (1983) Israel J Chem 23: 155

[6] a) *Kratky C, Jorde C, Falk H, Thirring K* (1983) Tetrahedron 39: 1859; b) *Kratky C, Falk H, Zrunek U* (1985) Monatsh Chem 116: 607; c) *Kratky C, Falk H, Grubmayr K, Zrunek U* (1985) Monatsh Chem 116: 761
[7] a) *Zielinski TJ, Breen DL, Rein R* (1978) J Am Chem Soc 100: 6266; b) *Klopman G, Andreozzi P, Hopfinger AJ, Kikuchi O, Dewar MJS* (1978) J Am Chem Soc 100: 6267
[8] *Falk H, Muller N* (1983) Tetrahedron 39: 1875
[9] *Martin GJ, Martin ML, Odiot S* (1975) Org Magn Reson 7: 2
[10] *Sterk H, Fabian W* (1975) Org Magn Reson 7: 274
[11] *Falk H, Müller N* (1985) Magn Reson Chem 23: 1353
[12] *Falk H, Müller N, Vormayr G* (1984) Org Magn Reson 22: 576
[13] *Dewar MJS, Thiel W* (1977) J Am Chem Soc 99: 4907
[14] *Vallès A* (1983) Tesi doctoral. Universitat de Barcelona
[15] *Mercè R, Pujol M, Ribó JM, Trull FR, Valera G, Vallès A* (1986) Monatsh Chem 117: 631
[16] *Falk H, Grubmayr K, Magauer K, Müller N, Zrunek U* (1983) Israel J Chem 23: 187
[17] *Bonfiglio JV, Bonnett R, Hursthouse MB, Abdul Malik KM, Naithani SC* (1977) JCS Chem Comm 1977: 829
[18] *Falk H, Müller N, Schlederer T* (1980) Monatsh Chem 111: 159
[19] *Falk H, Lehner F, Rothböck M* (1980) Monatsh Chem 116: 1359
[20] *Falk H, Zrunek U* (1984) Monatsh Chem 115: 101
[21] *Shorter J* (1973) Correlation analysis in organic chemistry: an introduction to LFER. Appendix. Clarendon Press, Oxford
[22] *Falk H* (1985) In: *Blauer G, Sund H* (eds) Optical properties and structure of tetrapyrroles. Walter de Gruyter, Berlin, p 281
[23] *Bois-Choissy M, Barbier M* (1978) Heterocycles 9: 677
[24] *Falk H, Müller N, Wansch S* (1985) Monatsh Chem 116: 1087
[25] *Falk H, Vormayr G, Margulies L, Metz S, Mazur Y* (1986) Monatsh Chem 117: 849